Journal of
Ceramic Science
and Technology

J. Ceram. Sci. Tech., **03** [03] 111-118 (2012)
DOI: 10.4416/JCST2012-00008
available online at: http://www.ceramic-science.com

Processing, Microstructure and Properties of Paper-Derived Porous Al_2O_3 Substrates

C. Kluthe [*1], B. Dermeik [2], W. Kollenberg [1], P. Greil [2], N. Travitzky [2]

[1]Department of Natural Science, Bonn-Rhein-Sieg University of Applied Sciences, von-Liebig-Str. 20, 53359 Rheinbach, Germany
[2]Department of Materials Science and Engineering (Glass and Ceramics), University of Erlangen-Nuremberg, Martensstr. 5, 91058 Erlangen, Germany
received March 23, 2012; received in revised form June 20, 2012; accepted June 27, 2012

Abstract

In this work, preceramic papers containing 85 wt% Al_2O_3 were heat-treated at 1600 °C to obtain paper-derived ceramics. In order to increase the preceramic paper density prior to sintering, the papers were calendered at different roll temperatures and pressures. The influences of the calendering parameters on the microstructure and mechanical properties of the preceramic papers and the paper-derived ceramics were investigated. It was expected that especially the mechanical properties of the papers and derived ceramics would be improved by calendering.

The increase in the preceramic paper density led to an increase by ~ 85 % of the green tensile strength from ~ 20 MPa to ~ 37 MPa in cross direction (CD) and by ~ 91 %, from ~ 11 MPa to ~ 21 MPa in machining direction (MD). An increase in flexural strength by ~ 96 %, from ~ 138 MPa to ~ 270 MPa, was obtained for the paper-derived ceramics with an increase in density by ~ 25 %, from ~ 2.4 g/cm³ to ~ 3.0 g/cm³, and the shrinkage after sintering was reduced from ~ 15 % to ~ 12 % owing to the previous calendering of the preceramic paper.

Keywords: Preceramic paper, calendering, mechanical properties, sintering, porosity

I. Introduction

Over the past several years, preceramic papers and the resulting ceramics (paper-derived ceramics) have received research attention [1–3]. Preceramic papers can be shaped in different ways, such as by laser cutting or laminated object manufacturing (LOM) [4,5]. When these paper sheets are heated, finished ceramics in the preset shape are obtained. The cellulose fibers decompose during the heat treatment and any remaining organic content is removed from the paper (at 300 – 800 °C). The inorganic content is consolidated by sintering [2].

The fabrication of preceramic papers is similar to the production of common writing paper. Both papers consist of cellulose fibers and inorganic fillers. These fillers are powdered minerals (e.g. kaolin and talc) or synthetic powders (e.g. $CaCO_3$ or TiO_2). However, the content of inorganic filler is significantly increased for the production of preceramic paper. The differences in composition between conventional writing paper and preceramic paper are shown in Table 1.

Organic fibers and inorganic fillers are mixed into water for preparing the preceramic paper suspension. The inorganic filler is expected to have a particle size of below 30 μm to avoid powder sedimentation during the production process [6]. In addition to the main components, coagulation and flocculation agents are added to the preceramic paper suspension. The suspension is then fed into a paper machine, which produces a continuous sheet of preceramic paper by a dewatering process (see [2] for technical details).

Table 1: Compositions of different types of papers

	Common writing paper	Al_2O_3-filled preceramic paper
Filler content /wt%	20 – 30	85
Mean particle size /μm	0.5 – 2	< 30
Sheet thickness /μm	110	750
Area density /g/m²	80	1000

The finished preceramic paper can be further processed in the calender. A calender applies a defined line load on the processed paper sheet by the pressure of its rolls. A defined calendering temperature is set by heating the calender rolls. The purpose of this work was to study the mechanical properties of the preceramic paper and of the paper-derived Al_2O_3-ceramic at different calendering temperatures and line loads. Also, the degree of material densification and surface smoothening was monitored for both materials.

* Corresponding author: christopher.kluthe@h-brs.de

II. Experimental

A laboratory calender (CA5/250 – 150 – 20, Sumet Messtechnik, Peiting, Germany), with a roll width of 200 mm and a roll diameter of 150 mm, was employed for calendering the preceramic papers. In the case of this study, a calender with two hardened and polished steel rolls was used (also referred to as hard calender nip). The calendering speed was kept at 0.5 m/min for all the preceramic paper samples. Thereby, the samples were calendered at different temperatures and roll pressures. The roll pressure is given as the line load applied perpendicular to the calendering direction [7–10]. The parameter range comprised eight line loads (10, 30, 50, 75, 100, 150, 200 and 250 kN/m) and four temperatures (25, 50, 75 and 100 °C), which resulted in 32 parameter combinations. The preceramic paper was calendered perpendicular to the machining direction.

Non-refined hardwood pulp (average diameter: 15 μm, average length: 657 μm, Celbi PP, Cellulose Beira Industrial (Celbi) S.A., Figueira da Foz, Portugal) [11] was used for the production of preceramic papers. Cellulose fibers constituted ~ 15 wt% of the paper. A bimodal alumina powder with primary grain sizes of 0.5 μm and 2 μm (Nabalox 625 – 31, Nabaltec AG, Schwandorf, Germany) made up ~ 80 wt% of the paper. Additionally, the paper contained ~ 3 wt% latex, ~ 1 wt% cationic starch and ~ 1 wt% polyacrylamide.

For the measurements on green paper, rectangular-shaped test specimens were cut out of paper samples calendered at different parameters. The thickness reduction owing to calendering was measured with a dial gauge (Käfer Messuhrenfabrik GmbH & Co. KG, Villingen-Schwenningen, Germany) at three different points on the sample. The green paper density was determined with the Archimedes method and the green tensile strength of the preceramic papers was measured with a universal mechanical testing machine (Instron 5565, Instron Engineering Cooperation, Norwood, USA).

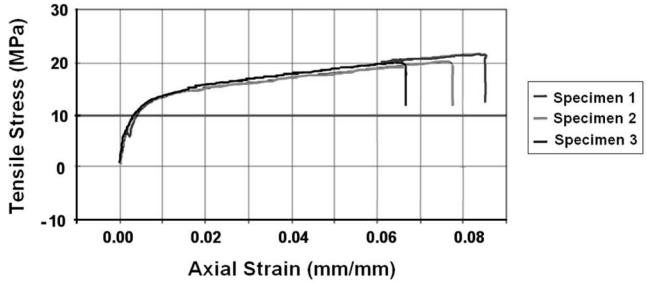

Fig. 1: Three typical curves from the tensile stress measurement of preceramic paper (calendering temperature: 100 °C, line load: 250 kN/m).

For green tensile strength tests, the measurement setup was adapted from EN ISO 1924 – 2 [12]. Test specimens of preceramic paper with 15 ± 1 mm in width and 105 ± 1 mm in length were used for the measurements. The test specimens were inserted into flat grips on both ends. Each grip covered an area of 30 x 15 mm² on the end of the test specimen, while the tensile stress was applied on an area of 45 x 15 mm². The test specimens were pulled at a constant elongation rate of 20 mm/min, while the strain was monitored with a video extensometer. Representative stress-strain curves are shown in Fig. 1. The green tensile strength of the samples was determined based on the maximum tensile stress value the samples could withstand, shortly before breaking. The measurements were repeated with six test specimens of each preceramic paper sample.

For each sintering experiment, one rectangular specimen (80 x 40 mm²) and five circular specimens (diameter: 9 mm) were used. These specimens were sintered at 1600 °C with a dwell time of 2 h. The shrinkage after sintering and the apparent density (Archimedes method) were measured for the sintered rectangular samples. The circular samples were used to determine the flexural strength of the ceramics by a ball-on-3-balls test (B3B – test) [13, 14]. In contrast to the 3- or 4-point flexural tests, which cause a uniaxial stress distribution within the test specimens, the B3B-test causes a biaxial stress distribution. The biaxial stress distribution has the advantage that loading of the edges of the brittle test material can be avoided and that the out-of-flatness of the test specimens can be neglected [14]. The flexural strength was calculated according to Eq. (1).

$$\sigma_m = f \cdot \frac{F}{t^2} \tag{1}$$

where,

σ_m: flexural strength (in MPa)
f: geometry factor (dimensionless)
F: bending force (in N)
t: thickness of the sample (in mm)

f is a geometrical factor and is calculated according to Eq. (2) [13].

$$f(\alpha, \beta, \mu) = c_0 + \left[\frac{c_1 + c_2\alpha + c_3\alpha^2 + c_4\alpha^3}{1 + c_5\alpha} \cdot (1 + c_6\beta) \right] \tag{2}$$

where,

$c_{0,1,2,3,4,5,6}$: specific constants for the material (dimensionless)
ν: Poisson's ratio of the material (dimensionless)
t: sample thickness (in mm)
R_s: radius of support (in mm)
R_d: disc radius (in mm)

The quantities α and β are defined as length ratios:

$\alpha = \frac{t}{R_d}$: ratio of sample thickness to the disc radius (dimensionless)

$\beta = \frac{R_s}{R_d}$: ratio of the radius of support to the disc radius (dimensionless)

The flexural strength of the paper-derived ceramic was measured with a universal mechanical testing machine (TIRAtest 2850, Tira GmbH, Schalkau, Germany). Scanning electron microscope (SEM) analysis and backscattered electrons (BSE) analysis were performed for the calendered preceramic paper specimens and the sintered, paper-derived ceramics (ESEM, Quanta 200, FEI s.r.o., Brno, Czech Republic and ESEM, JSM-6460, Jeol Ltd., Akishima, Japan).

III. Results and Discussion

(1) Properties of preceramic paper

Bar plots are used to display the monitored physical quantities of the preceramic paper samples plotted versus the line load, p, for different temperatures, T. The values of uncalendered samples are displayed as horizontal bars drawn in light gray shading. The thickness of the horizontal bars for the uncalendered paper samples reflects the measurement accuracy. All of the samples were calendered at a machine speed of 0.5 m/min, which was slow compared to machine speeds for common writing paper described in literature (> 75 m/min) [7–9].

The thickness reduction of the preceramic papers, at different calendering parameters, is shown in Fig. 2. The uncalendered preceramic paper characterized in this work had a thickness of 0.74 ± 0.02 mm. With an increase in the line load to 250 kN/m and at the calendering temperature of 25 °C, the paper thickness could be reduced by 20.3 ± 2.5 % to 0.59 ± 0.02 mm. With increasing calendering temperature, the thickness reduction is enhanced. At a line load value of 250 kN/m and at 100 °C the paper thickness reduction is 26.6 ± 2.5 %. Therefore, the line load is the most dominating parameter for the paper thickness reduction.

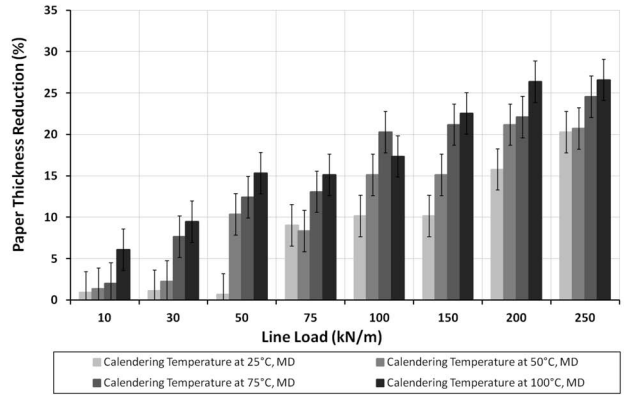

Fig. 2: Thickness reduction of the preceramic paper as a result of calendering.

The effect of calendering parameters on the paper density is shown in Fig. 3. The measured density of the uncalendered preceramic paper was 1.40 ± 0.01 g/cm³. When calendered at a line load of 250 kN/m at 100 °C, the paper density increased to 1.93 ± 0.01 g/cm³ (Fig. 3a). It was observed that the calendered papers elongated to up to ~ 3 % of the original length in CD, which was also the calendering direction, while no changes were observed for the paper length in MD. This means that the porosity of the paper decreased as a result of calendering, while the paper length was kept almost constant. A correlation plot between the density and the reduction of the paper thickness (Fig. 3b) proves the direct proportion between the both quantities. Eq. (3) gives the correlation equation obtained between the paper density and the paper thickness reduction.

$$y = 52.64\ x - 73.37 \qquad (3)$$

where,
x: preceramic paper density (in g/cm³)
y: paper thickness reduction (in %)

SEM micrographs of the cross-sections of green preceramic paper samples are shown in Fig. 4. The pore distribution inside the uncalendered green paper sample (Fig. 4a) is homogeneous over the area of the cross-section. The densification of sample calendered at maximum parameters (Fig. 4b) is most pronounced near to the surfaces. Hereby, the pores close to the surfaces are less than within the bulk. The pronounced densification of the preceramic paper on the surfaces can be explained by glass-rubber transition effects occurring in papers during calendering with heat [7, 10]. The pulp fibers consist of lignin, hemicelluloses and amorphous cellulose. When the calender temperature reaches the relaxation temperatures of these biological polymers, they become rubbery and flow more readily [15]. The intensified surface smoothening of the preceramic papers calendered at 250 kN/m (Fig. 4b) stems from the enlarged area of contact between the heated rolls and the paper. The enlarged area of contact gives rise to enhanced heat transfer from the calender rolls to the paper. Therefore, the influence of the calendering temperature on the paper properties becomes more significant with increasing line loads.

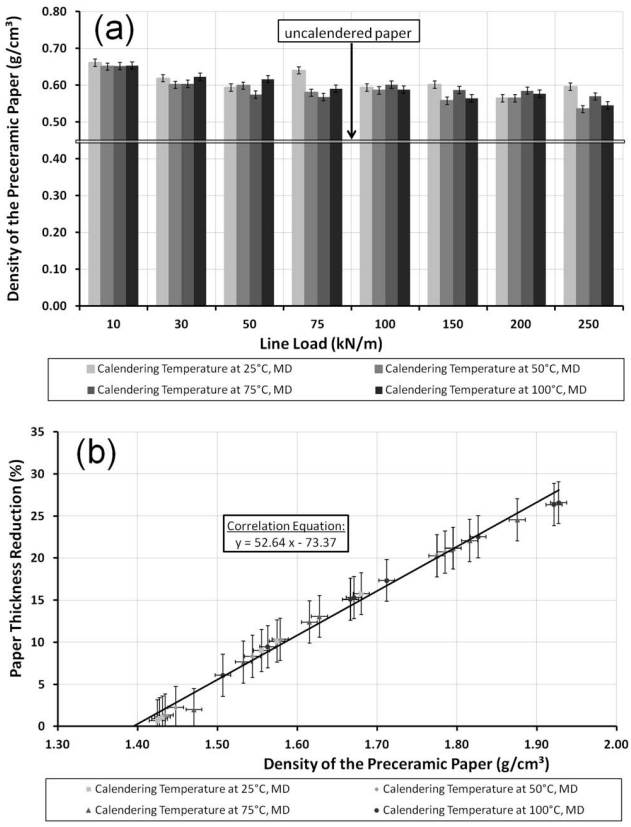

Fig. 3: Density values for the calendered preceramic paper compared to the uncalendered paper (a) and the correlation of the paper thickness reduction with the paper density (b).

The results of the tensile tests are presented in Fig. 5. The green tensile strength of the uncalendered preceramic paper was 20.3 ± 1.4 MPa in MD and 10.9 ± 1.3 MPa in CD. For the paper calendered at a line load of 250 kN/m and a temperature of 25 °C the green tensile increases to 31.9 ± 1.3 MPa in MD (Fig. 5a) and 17.5 ± 0.8 MPa in CD (Fig. 5b). At 250 kN/m and 100 °C, the green tensile strength further increases to 37.0 ± 2.1 MPa in MD and 20.6 ± 1.0 MPa in CD. The highest value for the green ten-

sile strength, of 21.1 ± 1.2 MPa, in CD is obtained for the parameters 250 kN/m and 75 °C. The increase in the green tensile strength of the samples after calendering compared to the uncalendered paper is given in Fig. 5c. The percentage increase of the green tensile strength is plotted versus the line load for different calendering temperatures. At the maximum line load value of 250 kN/m, the increase in green tensile strength ranges from 12.2 ± 1.2 % at 25 °C (in MD) to 93.4 ± 4.0 % at 75 °C (in CD). The increase in green tensile strength has similar slopes for all the applied calendering temperatures for samples in CD and in MD.

The pulp fibers at the surfaces of the preceramic paper, before and after calendering at the maximum parameter values (250 kN/m, 100 °C), are shown in Figs. 6 and 7. The most obvious feature is that the pulp fibers at the surfaces of the uncalendered paper sample are exposed. In contrast, the calendering caused the fibers to be embedded into the filler material. Furthermore, the pulp fibers cracked along their length direction. These cracks may originate from internal gaps the fibers received during calendering (Fig. 7). It is known that cellulose molecules within the pulp fibers are arranged in a helical structure. Slip planes can form in the fibers, as soon as they are plasticized by flexural or compressive forces [2, 16]. The cracks in the damaged pulp fibers of calendered preceramic paper can be expected to influence the mechanical properties of the paper owing to the disturbance of the plastification behavior. As discussed in [17], the highest nominal stresses in a bent paper are at the paper surfaces. Therefore, the flexural rigidity of the preceramic paper is expected to be affected owing to the damaged pulp fibers on the paper surface.

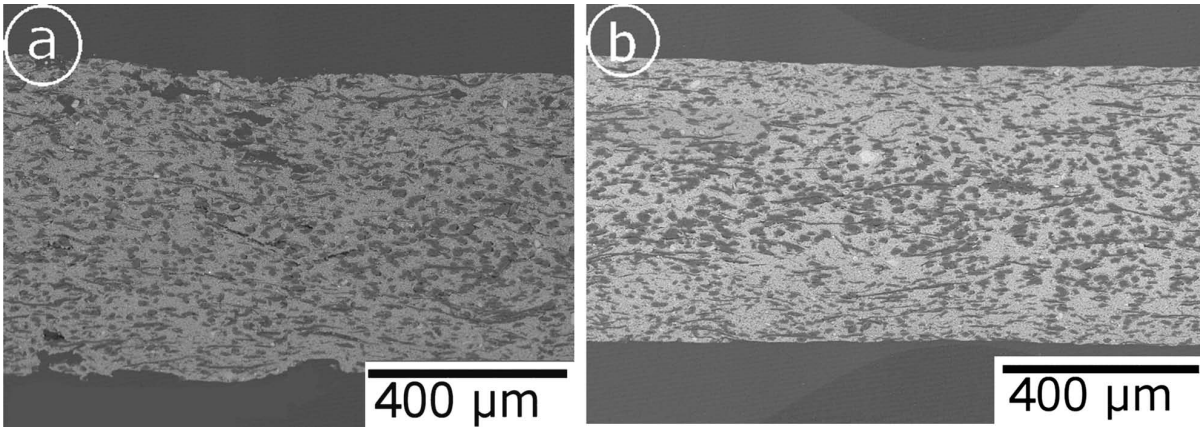

Fig. 4: Lateral SEM micrographs of an uncalendered preceramic paper (a) and a preceramic paper calendered at maximum parameter values (100 °C, 250 N/mm) (b).

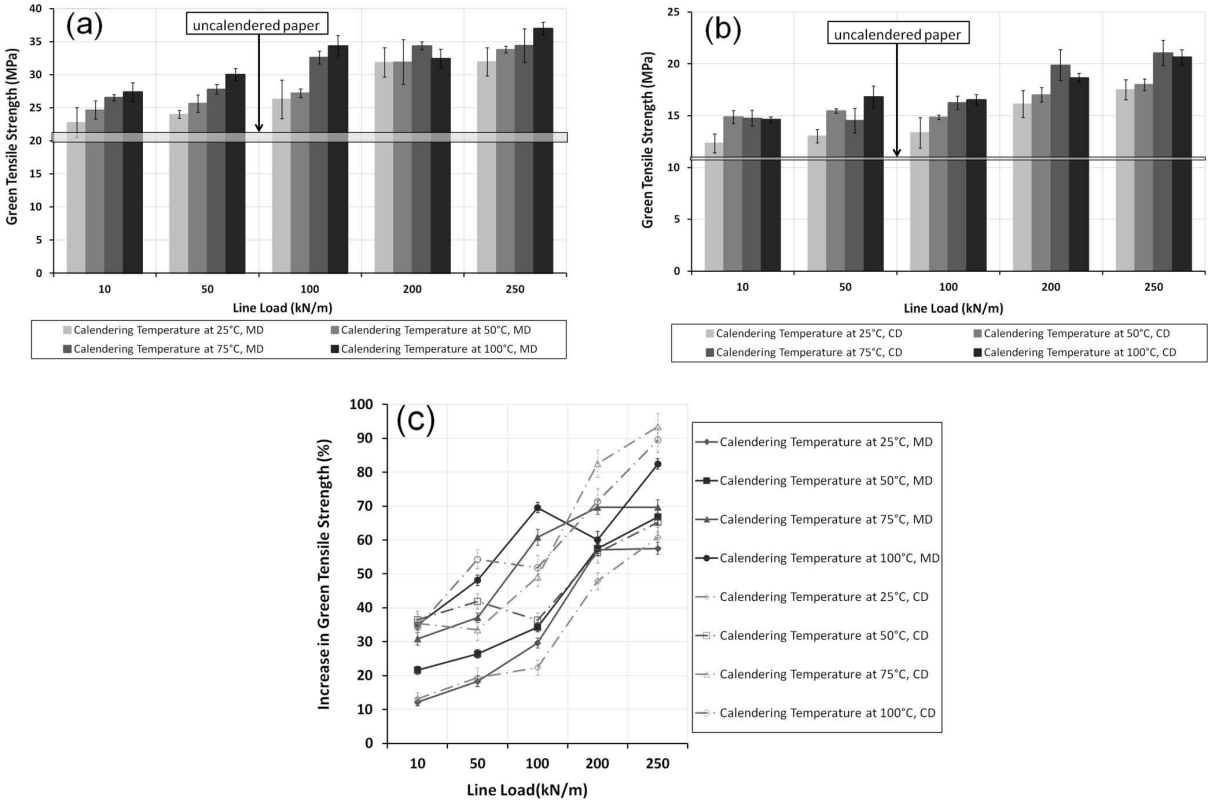

Fig. 5: Green tensile strength values of the calendered paper samples loaded in MD (a), in CD (b) compared to the uncalendered paper and the increases in green tensile strength for all the samples examined, CD and MD (c).

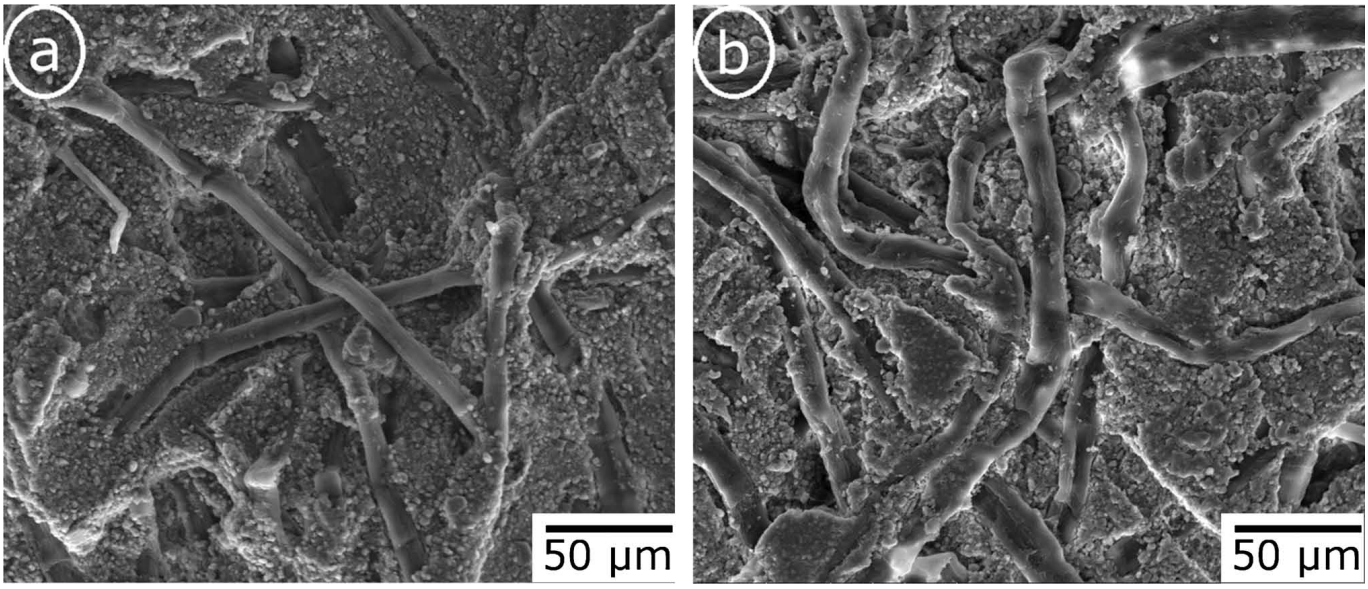

Fig. 6: SEM micrographs of the felt side (a) and the wire side (b) of an uncalendered preceramic paper.

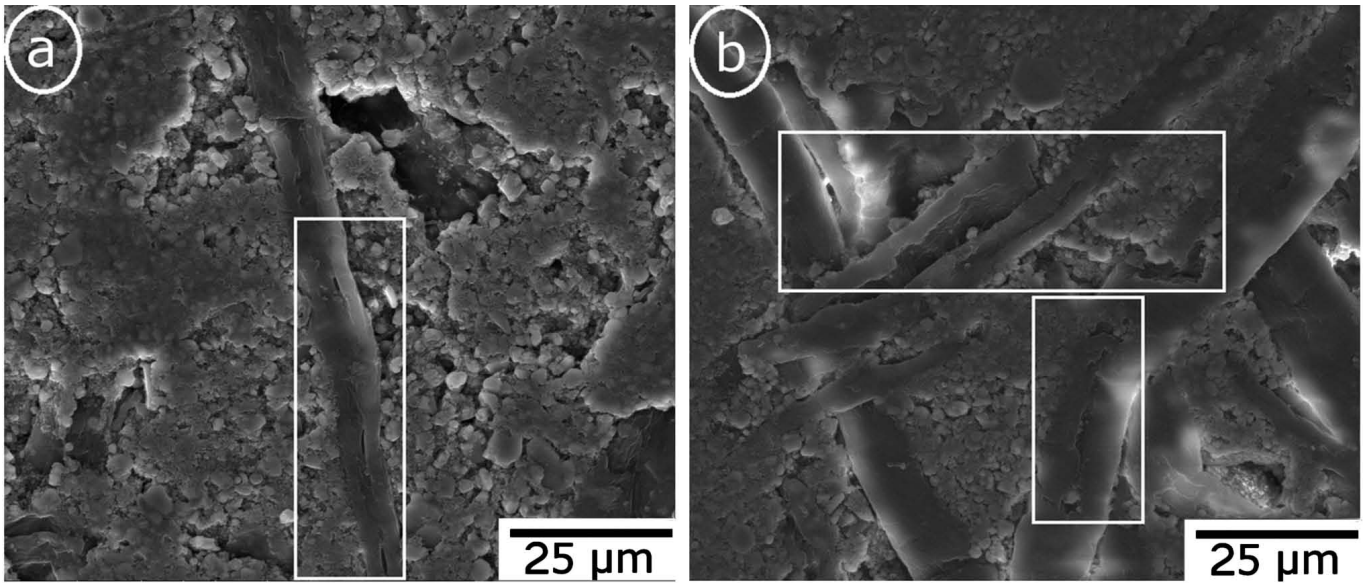

Fig. 7: SEM micrographs of the felt side (a) and the wire side (b) of a preceramic paper calendered at the maximum parameter values (100 °C, 250 kN/m).

(2) Properties of paper-derived ceramics

The influence of calendering on the sintering of the paper-derived ceramic was examined by measuring the material density. The results are presented in Fig. 8. The density of the ceramic derived from the uncalendered preceramic paper is 2.20 ± 0.01 g/cm³. When the maximum line load of 250 kN/m is applied to the preceramic paper, the density of the paper-derived ceramic is increased to 2.77 ± 0.01 g/cm³ at 25 °C and 3.02 ± 0.01 g/cm³ at 100 °C.

The sintering shrinkage of the paper-derived ceramic is effectively lowered by calendering. This is triggered by the decrease in the paper porosity. The shrinkage values, averaged from the shrinkages measured in MD and in CD, are presented in Fig. 9. The uncalendered preceramic paper shrunk at 15.0 ± 0.4 % when fired at 1600 °C for 2 h. It is shown that the shrinkage is reduced to 13.8 ± 0.3 % at the calendering temperature of 25 °C and the maximum line load value of 250 kN/m. At 100 °C, the shrinkage decreases further to 12.0 ± 0.3 %. The dependence between shrinkage, porosity and pore size also has been described in the literature [18,19].

The flexural strength values of the paper-derived ceramics, obtained with the B3B-test, are shown in Fig. 10. The flexural strength of the ceramic derived from the uncalendered paper is 138.3 ± 17.2 MPa. With application of the line load of 250 kN/m on the preceramic papers at 25 °C, the flexural strength of the paper-derived ceramics can be raised to 241.2 ± 6.7 MPa. Increasing the calendering temperature to 100 °C at 250 kN/m causes the flexural strength of the ceramics to increase to 265.8 ± 17.8 MPa. The highest value for the flexural strength, that is 298.2 ± 30.9 MPa, is obtained with the parameters 250 kN/m and 75 °C. Similarly to the results for the density and the shrinkage of the paper-derived ceramic, the flexu-

ral strength increases predominantly with increasing line loads. The observed increase in flexural strength is induced by the increase in density. This relation between the ceramic density and the flexural strength has been analyzed in previous works [20].

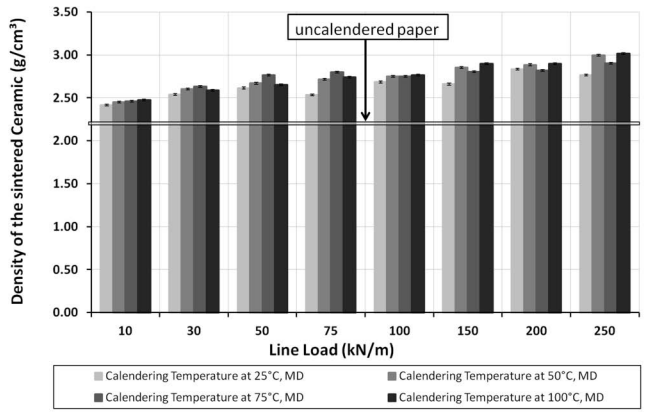

Fig. 8: Density values of the ceramics derived from calendered paper compared to the ceramics derived from uncalendered paper.

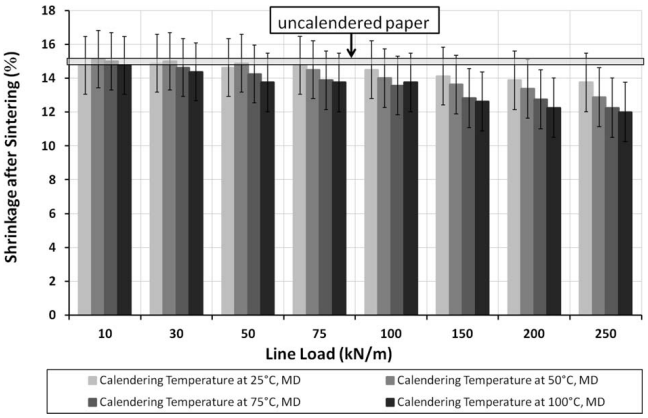

Fig. 9: Shrinkage after sintering of paper calendered with different sets of parameters compared to the shrinkage of uncalendered paper.

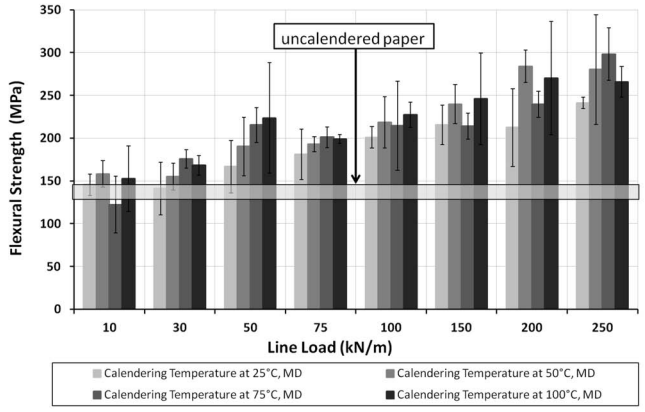

Fig. 10: Flexural strength values of the ceramics derived from calendered paper compared to the ceramics derived from uncalendered paper.

In order to examine the microstructure of the paper-derived ceramics, BSE micrographs were taken from cross-sections of the ceramics (perpendicular to the calendering direction) at four different sets of calendering parameters, combining the minimum and maximum values of the calendering temperature and the line load. The BSE micrographs are shown in Fig. 11. The samples calendered at the line load value of 10 kN/m (Fig. 11a and 11c) maintained a rough surface and a higher porosity compared to the samples calendered at 250 kN/m (Fig. 11b and 11d). The densification of the ceramic was influenced more predominantly by the line load at which the preceramic paper had been calendered than by the temperature. Two main types of pores are observed in paper-derived ceramics, i) elongated, anisotropic pores, formed by pyrolysis of the pulp fibers, and ii) pores originally present in the preceramic paper. Only the second type of pores, denoted as paper porosity, can be reduced by calendering [6]. Unlike in the case of the calendered green paper, the samples obtained from these papers show a homogeneous pore distribution all over the bulk material as well as near to the surface. Therefore, the bulk material of the calendered preceramic papers must have been densified during sintering. It is obvious that neither the line load, nor the calendering temperature has an effect on the pore distribution in the paper-derived ceramics.

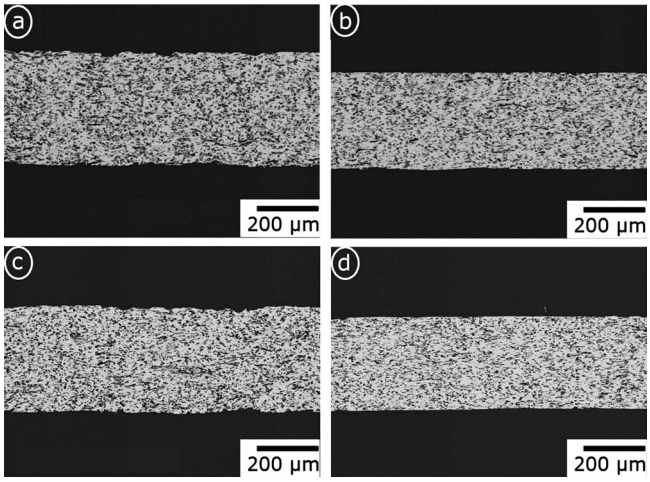

Fig. 11: Lateral BSE micrographs of the paper-derived ceramics with the paper calendered at 10 kN/m and 25 °C (a), at 250 kN/m and 25 °C (b), at 10 kN/m and 100 °C (c) as well as at 250 kN/m and 100 °C (d).

IV. Conclusions

The microstructure and mechanical properties of the preceramic paper, filled with Al_2O_3, and the paper-derived ceramic can be effectively controlled by calendering. The calendering influenced the microstructure and the mechanical properties in the following way:

- The green paper thickness could be reduced by ~ 27 %, from ~ 0.7 mm to ~ 0.6 mm.
- The green tensile strength of the preceramic paper could be increased by ~ 85 % in MD, from ~ 20 MPa to ~ 37 MPa, and by ~ 93 % in CD, from ~ 11 MPa to ~ 21 MPa.
- The density of the preceramic paper ceramics could be increased by ~ 38 %, from ~ 1.4 g/cm³ to ~ 1.9 g/cm³,

while density of the paper-derived ceramics could be increased by ~ 25 %, from ~ 2.4 g/cm³ to ~ 3.0 g/cm³.
- The shrinkage after sintering of the preceramic papers could be reduced from ~ 15 % to ~ 12 %.
- The flexural strength of the paper-derived ceramics could be increased by ~ 96 %, from ~ 138 MPa to ~ 270 MPa.

The process of calendering changes the morphology of the pulp fibers within the preceramic paper. A closer investigation of the calendered samples has shown that fibers on the paper surfaces crack when the paper is calendered.

Acknowledgement

The authors gratefully acknowledge the financial support by the DFG under the contract numbers KO 898/11 – 1 and TR 250/4 – 1.

References

1 Greil, P.: Biomorphous ceramics from lignocellulosics, *J. Eur. Ceram. Soc.*, **21**, 105 – 118, (2001).

2 Travitzky, N., Windsheimer, H., Fey, T., Greil, P.: Preceramic paper-derived ceramics, *J. Am. Ceram. Soc.*, **91**, 3477 – 3492, (2008).

3 Kollenberg W., Travitzky N.: PT-Ceramic: production and potential applications of ceramics created by paper technology, (in German), In: DKG-Handbuch: Technische Keramische Werkstoffe, HvB-Verlag, Ellerau, Chap. 4.9.1.0 1 – 21, (2010).

4 Weisensel, L., Travitzky, N., Sieber, H., Greil, P.: Laminated object manufacturing (LOM) of SiSiC composites, *Adv. Eng. Mat.*, **6**, 899 – 903, (2004).

5 Windsheimer, H., Travitzky, N., Hofenauer, A., Greil, P.: Laminated object manufacturing of preceramic-paper-derived si-siC composites, *Adv. Mater.*, **19**, 4515 – 4519, (2007)

6 Gutbrod, B., Haas, D., Travitzky, N., Greil, P.: Production of fireproof materials based on preceramic papers, (in German). In: DKG-Handbuch: Technische Keramische Werkstoffe, HvB-Verlag, Ellerau, Chap. 4.9.2.0 1 – 17, (2011) (And: DKG – Annual Meeting, Saarbruecken, Germany, 2011).

7 Enomae, T., Huang, T., LePoutre, P.: Softcalendering: effect of temperature, pressure and speed on sheet properties, *Nord. Pulp Pap. Res. J.*, **12**, 169 – 175, (1997).

8 Wikström, M., Nylund, T., Rigdahl, M.: Calendering of coated paper board in an extended soft nip, *Nord. Pulp Pap. Res. J.*, **12**, 289 – 298, (1997).

9 Granberg, A., Nylund, T., Rigdahl, M.: Calendering of a moistened woodfree uncoated paper, *Nord. Pulp Pap. Res. J.*, **3**, (1996).

10 Todorović, A., Hämäläinen, T.: Shoe nip calender possibilities for board and paper, In: Proceedings of the TAPPI spring technical conference, Chicago, (2003).

11 Gutbrod, B., Haas, D., Travitzky, N., Greil, P., Preceramic paper derived alumina/zirconia ceramics, *Adv. Eng. Mater.*, **13**, 494 – 501, (2011).

12 European Standard EN ISO 1924 – 2:2008, Paper and board – determination of tensile properties – Part 2: Constant rate of elongation method (20 mm/min).

13 Danzer, R., Harrer, W., Supancic, P., Lube, T., Wang, Z., Börger,A.: The ball on three ball test – strength and failure analysis of different materials, *J. Eur. Ceram. Soc.*, **27**, 1481 – 1485, (2007).

14 Börger, A., Supancic, P., Danzer, R.: The ball on three balls test for strength testing of brittle discs: stress distribution in the disc, *J. Eur. Ceram. Soc.*, **22**, 1425 – 1436, (2002).

15 Seth, R.S.: Understanding sheet extensibility, *Pulp Pap. – Canada*, **106**, 33 – 40, (2005).

16 Carlsson, L., Fellers, C., De Ruvo, A.: The mechanism of failure in bending of paperboard, *J. Mater. Sci.*, **15**, 2636 – 2642, (1980).

17 Roosen, A., Bowen, H.K.: Influence of various consolidation techniques on the Green. microstructure and sintering behavior of alumina powders, *J. Am. Ceram. Soc.*, **71**, 970 – 977, (1988).

18 Zheng, J., Reed, J.S.: Effects of particle packing characteristics on solid-state sintering, *J. Am. Ceram. Soc.*, **72**, 810 – 817, (1989).

19 Rice, W.R.: Evaluating porosity parameters for porosity-property relations, *J. Am Ceram. Soc.*, **76**, 1801 – 1808, (1993).

20 Paes, S.S., Shaomin, S., MacNaughtan, W., Ibbett, R., Ganster, J., Foster, T.J., Mitchell, J.R., The glass transition and crystallization of ball-milled cellulose, *Cellulose*, **17**, 693 – 709, (2010).